Geodynamics / Géodynamique

HP–LT Variscan metamorphism in the Cubito-Moura schists (Ossa-Morena Zone, southern Iberia)

Guillermo Booth-Rea [a,*], José Fernando Simancas [a], Antonio Azor [a], José Miguel Azañón [a], Francisco González-Lodeiro [a], Paulo Fonseca [b]

[a] *Departamento de Geodinámica, Universidad de Granada, 18071 Granada, Spain*
[b] *Departamento de Geologia, FCUL, Ed. C2, 5º Piso, Campo Grande, 1700 Lisboa, Portugal*

Abstract

Multi-equilibrium thermobarometry shows that low-grade metapelites (Cubito-Moura schists) from the Ossa–Morena Zone underwent HP–LT metamorphism from 340–370 °C at 1.0–0.9 GPa to 400–450 °C at 0.8–0.7 GPa. These HP–LT equilibriums were reached by parageneses including white K mica, chlorite and chloritoid, which define the earliest schistosity (S_1) in these rocks. The main foliation in the schists is a crenulation cleavage (S_2), which developed during decompression from 0.8–0.7 to 0.4–0.3 GPa at increasing temperatures from 400–450 °C to 440–465 °C. Fe^{3+} in chlorite decreased greatly during prograde metamorphism from molar fractions of 0.4 determined in syn-S_1 chlorites down to 0.1 in syn-S_2 chlorites. These new data add to previous findings of eclogites in the Moura schists indicating that a pile of allochtonous rocks situated next to the Beja-Acebuches oceanic amphibolites underwent HP–LT metamorphism during the Variscan orogeny. ***To cite this article: G. Booth-Rea et al., C. R. Geoscience 338 (2006).***

© 2006 Académie des sciences. Published by Elsevier Masson SAS. All rights reserved.

Résumé

Le métamorphisme varisque HP–BT des schistes de Cubito-Moura (zone d'Ossa Morena, Ibérie méridionale). La thermobarométrie utilisant l'équilibre local mica-chlorite ± chloritoïde montre que les métapélites de bas grade métamorphique (schistes de Cubito-Moura) de la zone d'Ossa Morena ont subi un métamorphisme de HP–BT de 340–370 °C à 1,0–0,9 GPa jusqu'à 400–450 °C à 0,8–0,7 GPa. Le pic du métamorphisme a été atteint aux plus basses pressions (approximativement de 0,8–0,7 GPa à 400–450 °C jusqu'à 0,4–0,3 GPa à 440–465 °C) durant la croissance de la foliation principale S_2 des métapélites. Le Fe^{3+} diminue largement dans les chlorites durant l'évolution métamorphique prograde, depuis des fractions molaires de 0,4 dans les chlorites de la schistosité S_1, jusqu'à 0,1 dans les chlorites de la foliation principale S_2. Ces nouvelles données s'ajoutent aux découvertes antérieures des éclogites dans les schistes de Moura, indiquant qu'un large volume de roches allochtones, situées à côté de l'unité des amphibolites océaniques de Beja-Acebuches, a subi un métamorphisme de HP–BT durant l'orogenèse varisque. ***Pour citer cet article : G. Booth-Rea et al., C. R. Geoscience 338 (2006).***

© 2006 Académie des sciences. Published by Elsevier Masson SAS. All rights reserved.

* Corresponding author.
  E-mail address: gbooth@ugr.es (G. Booth-Rea).

Version française abrégée

Introduction et cadre géologique

Dans le Sud-Ouest de l'Ibérie, la limite entre la zone d'Ossa Morena et la zone Sud-Portugaise est considérée comme la suture représentant la fermeture de l'océan Rhéïque (Fig. 1). Une unité amphibolitique d'affinité océanique marque ce contact tectonique majeur [4,5,9,11–13,25]. Un complexe de suture allochtone, moins bien connu, affleure au sud-ouest d'Ossa Morena (Fig. 1), au nord de la bande de l'amphibolite océanique, comprenant une large unité de métapélites (schistes de Cubito-Moura) et des affleurements épars d'éclogites et d'ophiolites en association avec des marbres [14]. La faible exposition et la déformation syn-collisionnelle sont parmi les raisons expliquant la connaissance insuffisante actuelle du complexe de la suture allochtone [2]. De plus, les techniques classiques de pétrologie métamorphique sont inadéquates pour détecter l'évolution HP des métapélites de grade métamorphique inférieur. Nous présentons ici les premiers résultats thermobarométriques des conditions $P–T$ subies par les schistes de Cubito-Moura, à partir de l'équilibre local des assemblages chlorite-micas-quartz $\pm$ chloritoïde.

Pétrographie et minéralogie

Les schistes de Cubito-Moura sont caractérisés par un clivage pénétratif de crénulation (S_2), qui constitue leur foliation principale (Fig. 2). Une schistosité antérieure est préservée dans des domaines lenticulaires du clivage S_2, principalement dans les lithologies riches en quartz (Fig. 3). Ces microstructures sont localement affectées par des plis asymétriques à vergence sud, associés à un clivage (S_3) de plan axial. Les paragenèses minérales présentes dans les schistes sont des assemblages à haute variance, formées de mica blanc potassique, de chlorite, de quartz, de tourmaline, $\pm$ magnétite, $\pm$ ilménite, $\pm$ rutile, $\pm$ paragonite, $\pm$ chloritoïde, $\pm$ albite, $\pm$ apatite, $\pm$ xénotime. Des cavités fibreuses à albite, apatite et oxydes de fer sont fréquemment observées dans des veines de quartz plissées et transposées par la foliation principale S_2 (Fig. 2A et B).

La composition des micas et des chlorites varie dans les différents domaines texturaux des échantillons étudiés. Dans les chlorites, une évolution générale est observée, depuis les compositions riches en clinochlore (0,11 Sud, 0,53 Clin et 0,36 Am), définissant S_1, jusqu'à des compositions riches en amésite (0,17 Sud, 0,37 Clin et 0,46 Am) dans la crénulation S_2. Les micas blancs potassiques (wKm) ont des teneurs en Si allant de 3,0 à 3,3 a.p.f.u. (Fig. 5A). La charge du cation interfoliaire, reliée à la substitution illitique, varie entre 0,84 et 0,94 (Fig. 5A). Les micas définissant la crénulation S_2 montrent des teneurs en cation interfoliaire plus élevées et un taux en Si plus faible que ceux préservées dans les domaines S_1.

Estimations thermobarométriques

Les conditions $P–T$ des paragenèses wKm + Chl + Qtz + W $\pm$ Ctd rencontrées dans les schistes de Cubito-Moura peuvent être calculées par thermobarométrie multi-équilibre [6] utilisant dix membres terminaux (eau, quartz, Mg-céladonite, muscovite, pyrophyllite, Mg-amésite, sudoïte, clinochlore, daphnite, Fe-céladonite et Mg-chloritoïde) dans le système KFMASH. Quatre-vingt-sept réactions peuvent être calculées dans le système KFMASH, cinq d'entre elles étant indépendantes (Fig. 3). Les estimations $P–T$ de ces réactions ont été calculé à l'aide du programme TWEEQ 1.02 [6], en utilisant la base de données JUN92, les propriétés thermodynamiques des dix membres terminaux et les modèles de solution solide mica–chlorite [23,26,30].

Les résultats thermobarométriques varient entre 340–370 °C à 1,0–0,9 GPa et 400–450 °C à 0,8–0,7 GPa pour les paragenèses mica–chlorite–chloritoïde définissant la foliation S_1 (Figs. 3 et 5B). Les conditions obtenues pour S_2 varient entre 400–450 °C à 0,8–0,7 GPa et 440–465 °C à 0,4–0,3 GPa (Figs. 3 et 5B).

Discussion et conclusions

L'équilibre local chlorite–micas–chloritoïde indique que les schistes de Cubito-Moura ont subi un événement métamorphique HP–BT à 340–450 °C et sous 1,0–0,7 GPa. Les résultats $P–T$ sont compatibles avec l'interprétation texturale que les cavités fibreuses observées dans les veines de quartz sont des pseudomorphes du carpholite, qui aurait été déstabilisé par le réchauffement tardif. Durant le métamorphisme HP–BT, les

schistes de Cubito-Moura ont subi un gradient métamorphique similaire à celui ayant affecté les éclogites du Sud du Portugal [14], suggérant que les schistes et les éclogites formaient une partie du même prisme orogénique. Un large volume de roches allochtones au sud-ouest d'Ossa Morena, au contact de la zone Sud-Portugaise, a donc subi un métamorphisme HP–BT durant l'orogenèse varisque. Ceci contraste avec l'évolution LP–HT de l'unité amphibolitique océanique de Beja-Acebuches [4], qui marque la limite entre ces zones.

1. Introduction and geological setting

Orogenic sutures are crucial for understanding the complexity of orogenic processes related to subduction,
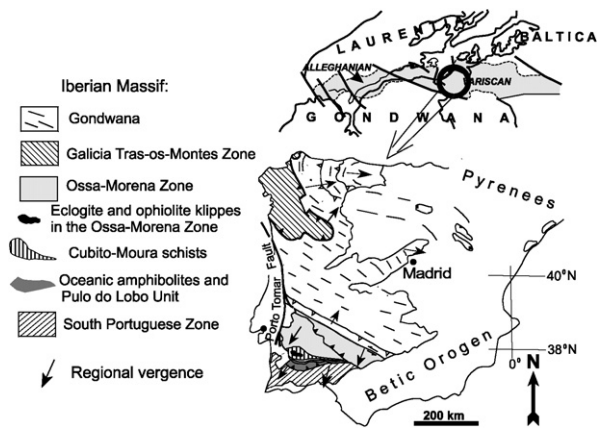

Fig. 1. Simplified geological sketch of the Iberian Peninsula showing the main zones and the location of the Cubito–Moura schists.

Fig. 1. Schéma géologique simplifié de la péninsule Ibérique, montrant les zones majeures et la localisation des schistes du Cubito–Moura.

obduction, and collision. In the Iberian Variscan Massif, suture terranes crop out at different tectonic settings. In northwestern Iberia, suture terranes are included in allochtonous units (the Galicia-Trás-Os-Montes Zone [3]) of uncertain rooting. In southwest Iberia, the boundary between the Ossa-Morena and the South Portuguese Zones is thought to be a suture, attesting the closure of the Rheic Ocean (Fig. 1). An amphibolitic unit, namely the Beja-Acebuches Amphibolites, marks this major tectonic contact [4,5,11–13,25]. North of this amphibolitic unit, an allochtonous complex crops out. It includes a widespread metapelitic unit (Cubito-Moura schists) and discrete outcrops of eclogites and MORB metabasites, in association with marbles [14]. Poor exposure and overprinting related to syn-collisional deformation are the main reasons explaining the very recent characterization of this allochtonous suture-related complex [2]. Moreover, the unsuitability of classical techniques in metamorphic petrology to detect high-pressure evolution in low-grade metapelites has contributed to the limited knowledge of the tectonometamorphic evolution of this unit. We present here the first thermobarometric results obtained from the Cubito-Moura schists, which represent the metapelitic rocks of this suture-related complex. The $P–T$ conditions have been determined from local equilibriums of chlorite–mica–quartz $\pm$ chloritoid assemblages, grown in different microstructural domains.

2. Petrography

The Cubito-Moura schists are characterized by a penetrative crenulation cleavage (S_2) that forms their main foliation (Fig. 2A and B). A previous schistosity

Fig. 2. (**A**) Pre-S_2 quartz vein with fibre-shaped voids (carpholite pseudomorphs?). (**B**) The same type of quartz vein affected by a fold related to the main foliation (S_2).

Fig. 2. (**A**) Veine de quartz avec des cavités fibreuses, possibles pseudomorphes de la carpholite. (**B**) Les veines de quartz sont affectées par des plis serrés dont la crénulation S_2 constitue le plan axial.

is preserved in lenticular domains of the S_2 cleavage, especially in quartz-rich lithologies. S_2 microstructures are locally folded by asymmetric south-vergent folds with an associated spaced axial-plane crenulation cleavage (S_3). Mineral parageneses in the schists are high-variance assemblages formed by white K-mica, chlorite, quartz, tourmaline, magnetite, $\pm$ ilmenite, $\pm$ rutile, $\pm$ paragonite, $\pm$ chloritoid, $\pm$ albite, $\pm$ apatite, $\pm$ xenotime. Quartz veins transposed by the main foliation or in hinges of isoclinal folds associated with the main foliation show many fibre-shaped voids filled in with iron oxides or albite and apatite (Fig. 2A and B). No remains of the original fibrous mineral have been found. Albite and apatite commonly occur in late veins too, frequently retrogressing previous minerals. Paragonite and xenotime contents increase as well in the later fabrics, especially in post S_2 shear zones.

In this paper, we present the results obtained from two schist samples bearing chlorite, phengite, paragonite, chloritoid, quartz, and ilmenite (samples Ara28 and Ara15 located at UTM coordinates: 29S0619346/4212974 and 29S0708988/4204897, respectively). Chloritoid is pre- to syn-kinematic with respect to the

Fig. 3. TWQ local equilibrium examples obtained from mica + chlorite + chloritoid parageneses. Notice the two foliations, S_1 and S_2, defined by mica, chlorite and chloritoid. Numbers in the SEM image show the analyses done on samples Ara28 and Ara15.

Fig. 3. Équilibres TWEEQ pour les paragenèses mica–chlorite–chloritoïde. Remarquer les deux foliations S_1 et S_2 définies par ces minéraux. Les points des analyses faites sur les échantillons Ara28 et Ara15 sont indiqués sur l'image MEB.

S_2 foliation (Fig. 3). Chlorite-white K mica couples occur in both the S_1 and S_2 foliations, as well as in chloritoid pressure shadows. Late mica-chlorite growth is observed also retrogressing chloritoid crystals in the quartz-rich pre-S_2 domains (Fig. 3).

3. Mineralogy

Chlorite, white K mica and chloritoid analyses were performed with a Cameca electron microprobe at the University of Granada (15 kV, 10 nA, PAP correction procedure) using Fe_2O_3 (Fe), $MnTiO_3$ (Mn, Ti), diopside (Mg, Si), CaF_2 (F), orthoclase (Al, K), anorthite (Ca) and albite (Na) as standards. X_{Mg} in minerals is calculated as $X_{Mg} = Mg/(Mg + Fe^{2-} + Mn)$. The analytical spot-size diameter was routinely set at 5 μm keeping the same current conditions. Structural formulae were calculated on the basis of 14 (anhydrous) oxygens for chlorite, 11 oxygens for mica, and 12 oxygens for chloritoid.

Chlorite has Si-contents ranging from 2.54 to 2.66 a.p.f.u. with X_{Mg} of 0.35–0.59, and an octahedral summation of 5.6–5.9 a.p.f.u. According to Vidal and Parra [28], Vidal et al. [29] and Parra et al. [23], these variations can be explained in terms of (1) $FeMg_{-1}$ substitution between daphnite [Daph: $Fe^{2+}{}_5Al_2Si_3O_{10} \cdot (OH)_8$] and clinochlore [Clin: $Mg_5AlSi_3O_{10}(OH)_8$] end-members, (2) Tschermak substitution ($Al_2R^{2+}{}_{-1}$· Si_{-1}: TK) between clinochlore/daphnite and amesite [Am: $(Fe, Mg)_4Al_4Si_2O_{10}(OH)_8$], and (3) di-trioctahedral substitution ($Ł(Fe^{3+}, Al)_2R^{2+}{}_{-3}$: DT) between daphnite/clinochlore and sudoite [Sud: $Ł(Fe, Mg)_2$-$(Fe^{3+}, Al)_4Si_3O_{10}(OH)_8$]. The extent of these substitutions depends on the metamorphic conditions and the rock chemistry. In the same way, at fixed *P* and *T* conditions, these substitutions are constrained by the mineralogical assemblage [16–18,21,22,26]. Chlorite becomes richer in clinochlore and sudoite at decreasing temperatures, thus increasing Si and vacancies (Ł). This trend is consistent with the various published empirical thermometers based on Al^{IV} and vacancies (e.g., [10, 15]). A general trend is observed in the chlorites from syn-S_1 clinochlore-rich compositions, with molar proportions of 0.11 Sud, 0.53 Clin and 0.36 Am, to syn-S_2 amesite-rich compositions (0.17 Sud, 0.37 Clin and 0.46 Am) in sample Ara28.

Fe^{3+} in chlorites has been estimated by using two different equilibriums. The first one is an 'internal equilibrium' involving Daph, Clin, Fe-Am and Mg-Am end-members. Since only three of these four end-members are independent, this 'internal equilibrium' must be satisfied to obtain the same solid-solution free energy cal-
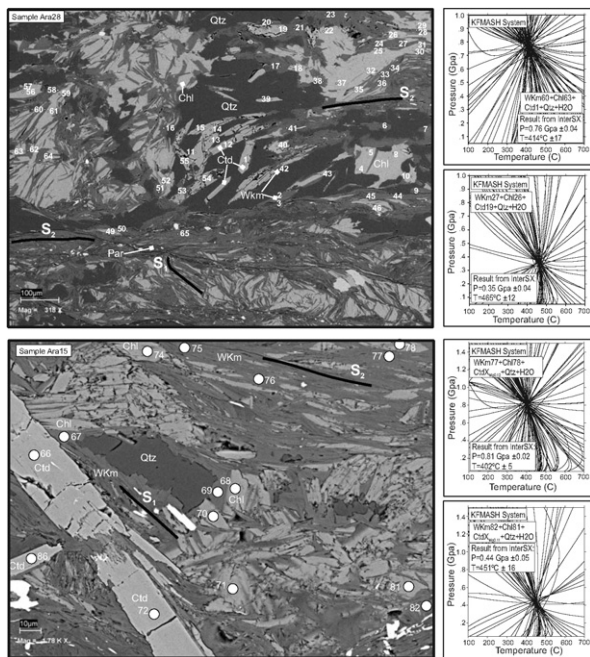
culated with either Clin, Daph, Fe- or Mg-Am [30]. The second equilibrium corresponds to Chl + Qtz (Clin + Sud = Mg-Am + Qtz + H_2O) (Fig. 4A). $X_{Fe^{3+}}$ varies among samples: in magnetite-rich ones, it ranges from 0.10 to 0.40, whilst in ilmenite-bearing samples (Ara28) it varies between 0.09 and 0.24. The highest Fe^{3+} content occurs in chlorites defining the S_1 foliation, located in the core of pre-S_2 quartz-rich domains, but sometimes too in post-S_2 shear planes.

White K-mica (wKm) has Si-contents ranging from 3.0 to 3.3 a.p.f.u. Variable Si-contents are generally interpreted in terms of Tschermak substitution alone (between celadonite and muscovite end-members), which

is favoured by a pressure increase [19,20]. However, this pressure-dependent substitution is not straightforward, because white K-micas show variable interlayer-cation contents together with a departure from the celadonite–muscovite binary. Interlayer-cation deficiency (interlayer sum ranges from 0.84 to 0.94 in the sample studied) has been attributed to the illite substitution in muscovite ($K^{XII}_{-1}Al^{IV}_{-1}Si^{IV}\square^{XII}$), which is favoured by decreasing temperatures [1,8,18,26]. The presence of smectite interlayers in the micas of the studied samples has been ruled out after XRD analysis. The <2-μm fraction was separated and analyzed with and without ethylene glycol treatment, to observe possible dif-
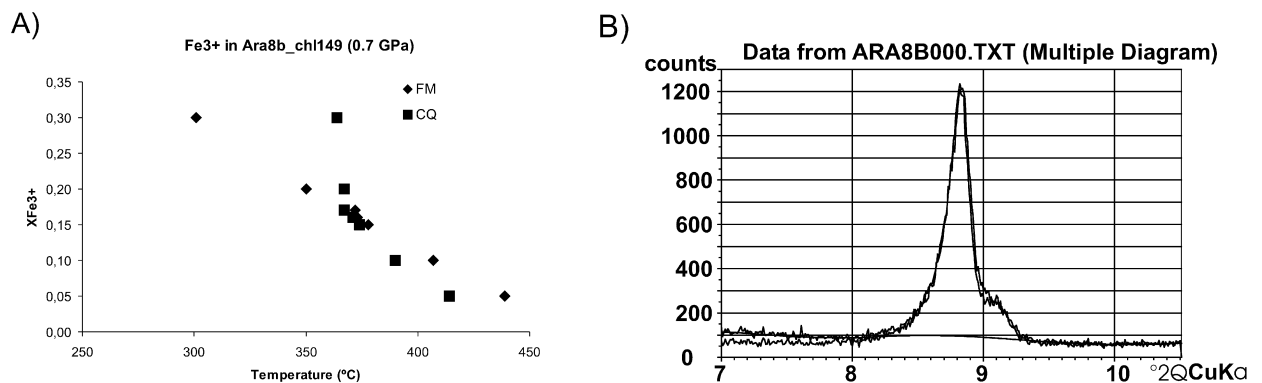

Fig. 4. (**A**) $X_{Fe^{3+}}$ versus temperature diagram used to estimate the Fe^{3+} content in chlorite by calibration using two reactions CQ (Clin + Sud = Mg-Am + Qtz + H_2O) and FM (Clin + 5 Fe-Am = 4 Daph + 5 Mg-Am). B. Two superposed XRD diagrams with the 10-Å peak of the <2-μm fraction from the studied sample before and after ethylene glycol treatment.

Fig. 4. (**A**) Diagramme $X_{Fe^{3+}}$ en fonction de la température, utilisé pour estimer la teneur en Fe^{3+} de la chlorite. Calibration avec les deux réactions CQ (Clin + Sud = Mg-Am + Qtz + H_2O) et FM (Clin + 5 Fe-Am = 4 Daph + 5 Mg-Am). (**B**) Superposition de deux diagrammes XRD du pic à 10 Å de la fraction <2 μm, avant et après traitement à l'éthylène glycol.
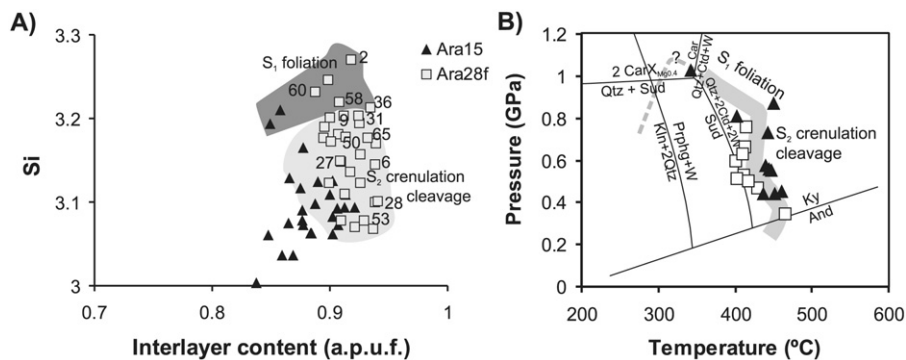

Fig. 5. (**A**) Composition of white K-micas in the sample studied expressed in a Si-Interlayer-Cation-content (IC) diagram. Notice the lower-Si and higher-IC content in the micas that define the main foliation relative to S_1 micas. Numbers in sample Ara28 refer to analyses shown in Fig. 3. (**B**) TWQ results of the studied samples showing HP–LT conditions obtained for the S_1 schistosity and later decompression during the growth of the S_2 main foliation. Standard mineral abbreviations.

Fig. 5. (**A**) Composition des micas-K, dans un diagramme des teneurs en Si et cations interfoliaires (IC). Notez la diminution de Si et l'augmentation de l'IC des micas S_2 par rapport aux micas marquant S_1. (**B**) Résultats TWEEQ pour l'échantillon étudié, montrant les conditions HP–BT obtenues pour la foliation S_1 et la décompression postérieure durant le développement de la crénulation S_2.

ferences in the 10- and 5-Å peaks in XRD diagrams after collapsing the hypothetical smectite layers. No differences were observed after ethylene glycol treatment (Fig. 4B). The micas defining the S_2 crenulation commonly show higher interlayer-cation contents and lower Si-contents than those preserved in the S_1 domains (Fig. 5A). $X_{Fe^{3+}}$ in white K-micas was estimated using the $K_{d_{Fe-Mg}}$ between mica and paragenetic chlorite, at the temperatures determined from chlorite + quartz equilibriums [28]. $X_{Fe^{3+}}$ in sample Ara28, which yielded the best results in our study, ranged between 0.3 and 0.6.

Chloritoid shows X_{Mg} varying between 0.13 and 0.11 in sample Ara15 and between 0.08 and 0.07 in sample Ara28.

4. Local-equilibrium thermobarometry

Multi-equilibrium thermobarometry [6] is appropriate in the particular case of mica–chlorite pairs, because the equilibration of these minerals at varying P and T is mostly achieved by crystallisation/recrystallisation processes rather than by changing the composition of older grains by lattice diffusion. This is the case at the low-temperature fields of blueschist and greenschist facies metamorphism. Moreover, the relative sequence of crystallization of phyllosilicates can frequently be determined by microstructural criteria. Thus, using chlorite–white K-mica pairs defining different microstructures in a metamorphic rock, one can determine the $P–T$ conditions under which each microstructure developed (e.g., [7,24]). The $P–T$ conditions for the paragenesis wKm + Chl + Qtz + H_2O ± Ctd found in the Cubito schists can be calculated using a number of phases and end-members (water, quartz, Mg-celadonite, muscovite, pyrophyllite, Mg-amesite, sudoite, clinochlore, daphnite, Fe-celadonite and Mg10 chloritoid) in the KFMASH system. Eighty-seven equilibriums can be determined with five independent reactions (Fig. 3). The $P–T$ location of these reactions was calculated with the TWQ 1.02 software [6] and its associated database JUN92, together with thermodynamic properties for the above end-members as well as chlorite and mica solid-solution models [23,27–30]. Ideally, all the equilibriums calculated for a given paragenesis should intersect at a single point. However, in practice, some scatter is commonly observed. The scatter results from errors in each reaction, which stem from the uncertainties in the thermodynamic properties of end members and solution models, departure of the analysed compositions from equilibrium compositions and analytical uncertainties. The character and magnitude of these uncertainties have

been discussed by Vidal and Parra [26]. Following these authors, the temperature (σ_T) and pressure (σ_P) scatter are calculated with INTERSX [6] and if $\sigma_P > 0.08$ GPa or $\sigma_T > 25\,°C$, the minerals are considered to be out of equilibrium and the $P–T$ estimates are rejected. Furthermore, we have only used equilibriums with a minimum of four independent reactions.

The thermobarometric results for sample Ara28 are of 380–440 °C at 0.8–07 GPa using mica–chlorite–chloritoid paragenesis defining the S_1 foliation (Figs. 3 and 5B). The conditions obtained from the paragenesis related to the S_2 crenulation cleavage range from 375–425 °C at 0.6–0.7 GPa to 440–465 °C at 0.3–0.4 GPa (Figs. 3 and 5B). $P–T$ conditions between 340–370 °C at 1.0–0.9 GPa and 425–450 °C at 0.9–0.8 GPa were obtained for S_1 growth in sample Ara15. The higher pressure obtained in this sample respect to Ara28, results from higher X_{Mg} in chloritoid, paragenetic with a low-temperature sudoite- and Si-rich chlorite. For S_2 TWQ results range between 400–440 °C at 0.8–0.7 GPa and 440–460 °C at 0.4–0.5 GPa. Chlorite + quartz equilibriums checked in other samples of Moura-Cubito schists indicate that these reached variable peak temperatures ranging between 400 and 465 °C, probably depending on their depth within the metamorphic pile.

5. Discussion and conclusions

Chlorite–mica–chloritoid local equilibriums indicate that the Cubito-Moura schists underwent HP–LT metamorphism during the growth of their S_1 schistosity that developed during heating and slight decompression between conditions of 340–370 °C at 1.0–0.9 GPa and 400–450 °C at 0.8–0.7 GPa. The S_2 main foliation developed during isothermal decompression, followed by slight heating during further decompression, from 400–450 °C at 0.8 to 0.5 GPa, to 440–465 °C at 0.3–0.4 GPa (Fig. 5B). The $P–T$ results obtained for the growth of the S_1 schistosity support the possibility that the fibre-like voids observed in quartz veins are pseudomorphs after carpholite, which would have been destabilised during later prograde metamorphism or by late sodium-rich fluids related with Carboniferous magmatism. $P–T$ conditions of 340–370 °C and 1.0–0.9 GPa determined for the most Mg-rich chloritoid in sample Ara15 fall on the carpholite ($X_{Mg} = 0.4$)–sudoite–chloritoid invariant point (Fig. 5B), suggesting that carpholite could have reacted to produce chloritoid + quartz + water. Fe^{3+} content in chlorite shows a clear textural control within samples, showing a decrease from $X_{Fe^{3+}} = 0.4$ in the pre-S_2 microstructural domains to values of $X_{Fe^{3+}} =$

0.1 in the S_2 foliation, thus indicating reduction in the redox state during prograde metamorphism.

During HP–LT metamorphism, the Cubito-Moura schists underwent a similar metamorphic gradient as the one observed in the eclogites of the southern Ossa-Morena Zone, though in these latter higher pressure conditions have been reported [14]. This fact suggests that these rocks, together with the eclogites, formed part of a thick orogenic wedge [2]. Remnants of this orogenic wedge crop out as a continuous allochtonous unit (Cubito and Moura schists, in Spain and Portugal, respectively) located in the southern part of the Ossa-Morena Zone, north of the boundary marked by the Beja-Acebuches amphibolites. Thus, in the boundary between the Ossa-Morena and South Portuguese zones, a pile of rocks underwent HP–LT metamorphism during the Variscan orogeny, though, by contrast, the nearby Beja-Acebuches oceanic amphibolites underwent a LP–HT evolution [4,9,11].

Acknowledgements

References

[1] P. Agard, O. Vidal, B. Goffé, Interlayer and Si content of phengite in HP–LT carpholite-bearing metapelites, J. Metamorph. Geol. 19 (2001) 477–493.

[2] A. Araújo, P. Fonseca, J. Munhá, P. Moita, J. Pedro, A. Ribeiro, The Moura phyllonitic complex: An accretionary complex related with obduction in the southern Iberia Variscan suture, Geodin. Acta 18 (2005) 375–388.

[3] R. Arenas, I. Gil Ibarguchi, F. González Lodeiro, E. Klein, J.R. Martínez Catalán, E. Ortega Gironés, J.G. Pablo Maciá, M. Peinado, Tectonostratigraphic units in the complexes with mafic and related rocks of the NW of the Iberian Massif, Hercynica 2 (1986) 87–110.

[4] J.-P. Bard, Signification tectonique des métatholeiïtes d'affinité abyssale de la ceinture métamorphique de basse pression d'Aracena (Huelva, Espagne), Bull. Soc. geol. France 19 (7) (1977) 385–393.

[5] J.-P. Bard, B. Moine, Acebuches amphibolites in the Aracena Hercynian metamorphic belt (southwest Spain): Geochemical variations and basaltic affinities, Lithos 12 (1979) 271–282.

[6] R.G. Berman, Thermobarometry using multi-equilibrium calculations: a new technique, with petrological applications, Can. Mineral. 29 (1991) 833–855.

[7] G. Booth-Rea, J.M. Azañón, J.M. Martínez-Martínez, O. Vidal, V. García-Dueñas, Contrasting structural and *P*–*T* evolutions of tectonic units in the southeastern Betics: key for understanding the exhumation of the Alboran Domain HP/LT crustal rocks (Western Mediterranean), Tectonics 24 (2005); doi:10.1029/2004TC001640.

[8] R. Bousquet, L'exhumation des roches métamorphiques de haute pression–basse température : de l'étude de terrain à la modélisation numérique. Exemple de la fenêtre de l'Engadine et du domaine Valaisan dans les Alpes centrales, PhD thesis, University Paris-11, France, 1998.

[9] A. Castro, C. Fernández, J.D. De la Rosa, I. Moreno Ventas, G. Rogers, Significance of MORB-derived amphibolites from the Aracena metamorphic belt, southwest Spain, J. Petrol. 37 (1996) 235–260.

[10] M. Cathelineau, D. Nieva, A chlorite solid solution geothermometer. The Los Azufres (Mexico) geothermal system, Contrib. Mineral. Petrol. 91 (1985) 235–244.

[11] A. Crespo-Blanc, Evolución geotectónica del contacto entre la Zona de Ossa-Morena y la Zona Sudportuguesa en la sierras de Aracena y Aroche (Macizo Ibérico meridional): un contacto mayor en la Cadena Hercínica europea, PhD thesis, Universidad de Sevilla, 1989.

[12] C. Dupuy, J. Dostal, J.-P. Bard, Trace-element geochemistry of Paleozoic amphibolites from SW Spain, Tschermaks Min. Petrol. Mitt. 26 (1979) 87–93.

[13] P. Fonseca, A. Ribeiro, Tectonics of the Beja-Acebuches ophiolite: a major suture in the Iberian Variscan Foldbelt, Geol. Rundsch. 82 (1993) 440–447.

[14] P. Fonseca, J. Munhá, J. Pedro, F. Rosas, P. Moita, A. Araújo, N. Leal, Variscan ophiolites and high-pressure metamorphism in southern Iberia, Ofioliti 24 (2) (1999) 259–268.

[15] S. Hillier, B. Velde, Octahedral occupancy and the chemical composition of diagenetic (low-temperature) chlorites, Clay Miner. 26 (1991) 146–168.

[16] T.J.B. Holland, J. Baker, R. Powell, Mixing properties and activity-composition relationships of chlorites in the system MgO–FeO–Al$_2$O$_3$–SiO$_2$–H$_2$O, Eur. J. Mineral. 10 (1998) 395–406.

[17] D.M. Jenkins, J.V. Chernosky, Phase equilibria and crystallo-chemical properties of Mg-chlorites, Am. Mineral. 71 (1986) 924–936.

[18] L. Leoni, F. Sartori, M. Tamponi, Compositional variation in K-white micas and chlorites coexisting in Al-saturated metapelites under late-diagenetic to low-grade metamorphic conditions (Internal Liguride Units, Northern Apennines, Italy), Eur. J. Mineral. 10 (1998) 1321–1339.

[19] H.J. Massonne, Experimental and petrogenetic study of UHPM, in: R.G. Coleman, X. Wang (Eds.), Ultra High Pressure Metamorphism, Cambridge University Press, Cambridge, UK, 1995, pp. 33–95.

[20] H.J. Massonne, W. Schreyer, Phengite geobarometry based on the limiting assemblage with K-feldspar, phlogopite and quartz, Contrib. Mineral. Petrol. 96 (1987) 214–224.

[21] H.J. Massonne, Z. Szpurka, Thermodynamic properties of white micas on the basis of high-pressure experiments in the systems K$_2$O–MgO–Al$_2$O$_3$–SiO$_2$–H$_2$O, Lithos 41 (1997) 229–250.

[22] D. McPhail, R.G. Berman, H.J. Greenwood, Experimental and theoretical constraints on aluminium substitutions in magnesian chlorite, and a thermodynamic model for H$_2$O in magnesian cordierite, Can. Mineral. 28 (1990) 859–874.

[23] T. Parra, O. Vidal, P. Agard, A thermodynamic model for Fe–Mg dioctahedral K-white micas using data from phase equilibrium experiments and natural pelitic assemblages, Contrib. Mineral. Petrol. 143 (2002) 706–732.

[24] T. Parra, O. Vidal, L. Jolivet, Relation between the intensity of deformation and retrogression in blueschist metapelites of Tinos Island (Greece) evidenced by chlorite-mica local equilibria, Lithos 63 (2002) 41–66.

[25] C. Quesada, P. Fonseca, J. Munhá, J.T. Oliveira, A. Ribeiro, The Beja–Acebuches ophiolite (southern Iberia, Variscan Foldbelt): geological characterization and geodynamic significance, Bol. Geol. Min. 105 (1994) 3–49.

[26] O. Vidal, T. Parra, Exhumation paths of high pressure metapelites obtained from local equilibria for chlorite–phengite assemblages, Geol. J. 35 (2000) 139–161.

[27] O. Vidal, B. Goffé, T. Theye, Experimental study of a new petrogenetic grid for the system $FeO–MgO–Al_2O_3–SiO_2–H_2O$, J. Metamorph. Geol. 14 (1992) 381–386.

[28] O. Vidal, B. Goffé, R. Bousquet, T. Parra, Calibration and testing of an empirical chloritoid-chlorite thermometer and thermodynamic data for daphnite, J. Metamorph. Geol. 10 (1999) 603–614.

[29] O. Vidal, T. Parra, F. Trotet, A thermodynamic model for Fe–Mg aluminous chlorite using data from phase equilibrium experiments and natural pelitic assemblages in the 100–600 °C, 1–25 kbar P–T range, Am. J. Sci. 301 (2001) 557–592.

[30] O. Vidal, T. Parra, P. Vieillard, Thermodynamic properties of the Tschermak solid solution in Fe-chlorite: Application to natural examples and possible role of oxidation, Am. Mineral. 90 (2005) 347–358.